nature chemistry

ARTICLES

PUBLISHED ONLINE: 14 JULY 2013 | DOI: 10.1038/NCHEM.1704

A grossly warped nanographene and the consequences of multiple odd-membered-ring defects

Katsuaki Kawasumi[1], Qianyan Zhang[2], Yasutomo Segawa[1], Lawrence T. Scott[2]* and Kenichiro Itami[1,3]*

Graphite, the most stable form of elemental carbon, consists of pure carbon sheets stacked upon one another like reams of paper. Individual sheets, known as graphene, prefer planar geometries as a consequence of the hexagonal honeycomb-like arrangements of trigonal carbon atoms that comprise their two-dimensional networks. Defects in the form of non-hexagonal rings in such networks cause distortions away from planarity. Herein we report an extreme example of this phenomenon. A 26-ring $C_{80}H_{30}$ nanographene that incorporates five seven-membered rings and one five-membered ring embedded in a hexagonal lattice was synthesized by stepwise chemical methods, isolated, purified and fully characterized spectroscopically. Its grossly warped structure was revealed by single-crystal X-ray crystallography. An independent synthetic route to a freely soluble derivative of this new type of 'nanocarbon' is also reported. Experimental data reveal how the properties of such a large graphene subunit are affected by multiple odd-membered-ring defects.

Modern nanocarbon science was born in 1985 when C_{60} and the higher fullerenes were discovered[1]. The field expanded rapidly and attracted even more widespread interest with the discovery of carbon nanotubes in 1991[2] and the subsequent isolation of single-layer graphene in 2004[3]. The hollow balls, long tubes and flat sheets of trigonal carbon atoms that make up these structurally distinct families of all-carbon molecules exhibit a range of remarkable properties that has spawned an ever-more intensifying revolution in materials science[4]. Herein we report a grossly warped nanographene, the first member of a new family of nanocarbons (Fig. 1a). This chiral, warped $C_{80}H_{30}$ nanographene, with five seven-membered rings and one five-membered ring embedded in a hexagonal lattice of trigonal carbon atoms, can be synthesized rapidly from commercially available corannulene in just two steps by C–H activation reactions[5,6]. A number of unique structural and physical properties were uncovered, such as facile bowl-to-bowl inversion of the central corannulene, a unique racemization pathway, high solubility in common organic solvents and a widened highest occupied molecular orbital (HOMO)–lowest unoccupied molecular orbital (LUMO) gap.

Since the early 1990s, we[7–10] and other chemists[11–13] have set our sights on developing new laboratory methods for the chemical synthesis of small, well-defined, carbon-rich compounds and nanocarbons, motivated partly by the desire to study their unique properties, but also as practice for synthesizing full-size, structurally uniform carbon materials 'from the ground up'. Large numbers of bowl-shaped fullerene fragments[7–14], circular nanotube sections[14–26] and disc-shaped graphene substructures[27–29] have now been prepared and studied. Even chemical syntheses that produce C_{60} (ref. 30) and the first structurally pure, short, rigid carbon nanotube[31] are reported, both in isolable quantities.

We have begun to develop methods for the rapid, controlled build-up of large graphene subunits from smaller molecular platforms. For this purpose, few methods have proved as powerful as our recently introduced palladium-catalysed biphenylation of polycyclic aromatic hydrocarbons (PAHs) through C–H activation followed by cyclodehydrogenation[32]. When this reaction sequence is applied to the bowl-shaped PAH corannulene (**1**), we found that it does not stop at the fivefold annulated product **3**, but continues all the way to the grossly warped $C_{80}H_{30}$ nanographene **4** (Fig. 1b). The cyclization reaction conditions append five polycyclic wings to the central hydrocarbon bowl and then stitch them together to create five new seven-membered rings. Ten new carbon–carbon bonds are formed in a single reaction.

The expansion of corannulene (**1**) to give the $C_{80}H_{30}$ nanographene **4** quadruples the number of atoms in the carbon lattice and increases the number of rings from six to 26 in just two steps. The lack of regioselectivity in the fivefold C–H arylation produces a mixture of products, which limits the yield in the first step of the synthesis, but the isomerically pure 1,3,5,7,9-pentakis(2-biphenylyl)corannulene (**6**) is accessible in high yield by a self-correcting, exhaustive C–H borylation of **1** (ref. 33), followed by a Suzuki–Miyaura coupling of the resulting 1,3,5,7,9-pentakis(Bpin)corannulene (**5**). Cyclodehydrogenation of intermediate **6** similarly produces **4** (Fig. 1b).

A third route to this highly contorted 80-carbon ring system through C–H activation was also developed (Fig. 1b). Thus, cyclodehydrogenation of decakis(4-*t*-butylphenyl)corannulene (**7**), which we recently synthesized directly from corannulene (**1**) by tenfold C–H arylation[34], gives the same 26-ring carbon framework in 62% yield, decorated now by ten *t*-butyl groups on the perimeter (**8**).

The strategy of stitching together phenyl groups or substituted phenyl groups by cyclodehydrogenation reactions has been used to produce many large, planar PAHs, especially during the past 10–15 years[27–29]. Much of the success in this chemistry can be attributed to the formation of strain-free six-membered rings from crowded starting materials. The formation of strained seven-membered rings by cyclodehydrogenation reactions, however, is almost unprecedented[35–37]. For example, we have already confirmed that [6]helicene does not undergo cyclodehydrogenation to form

[1]Department of Chemistry, Graduate School of Science, Nagoya University, Chikusa, Nagoya 464-8602, Japan, [2]Merkert Chemistry Center, Boston College, Chestnut Hill, Massachusetts 02467-3860, USA, [3]Institute of Transformative Bio-Molecules (WPI-ITbM), Nagoya University, Chikusa, Nagoya 464-8602, Japan. *e-mail: itami.kenichiro@a.mbox.nagoya-u.ac.jp; lawrence.scott@bc.edu

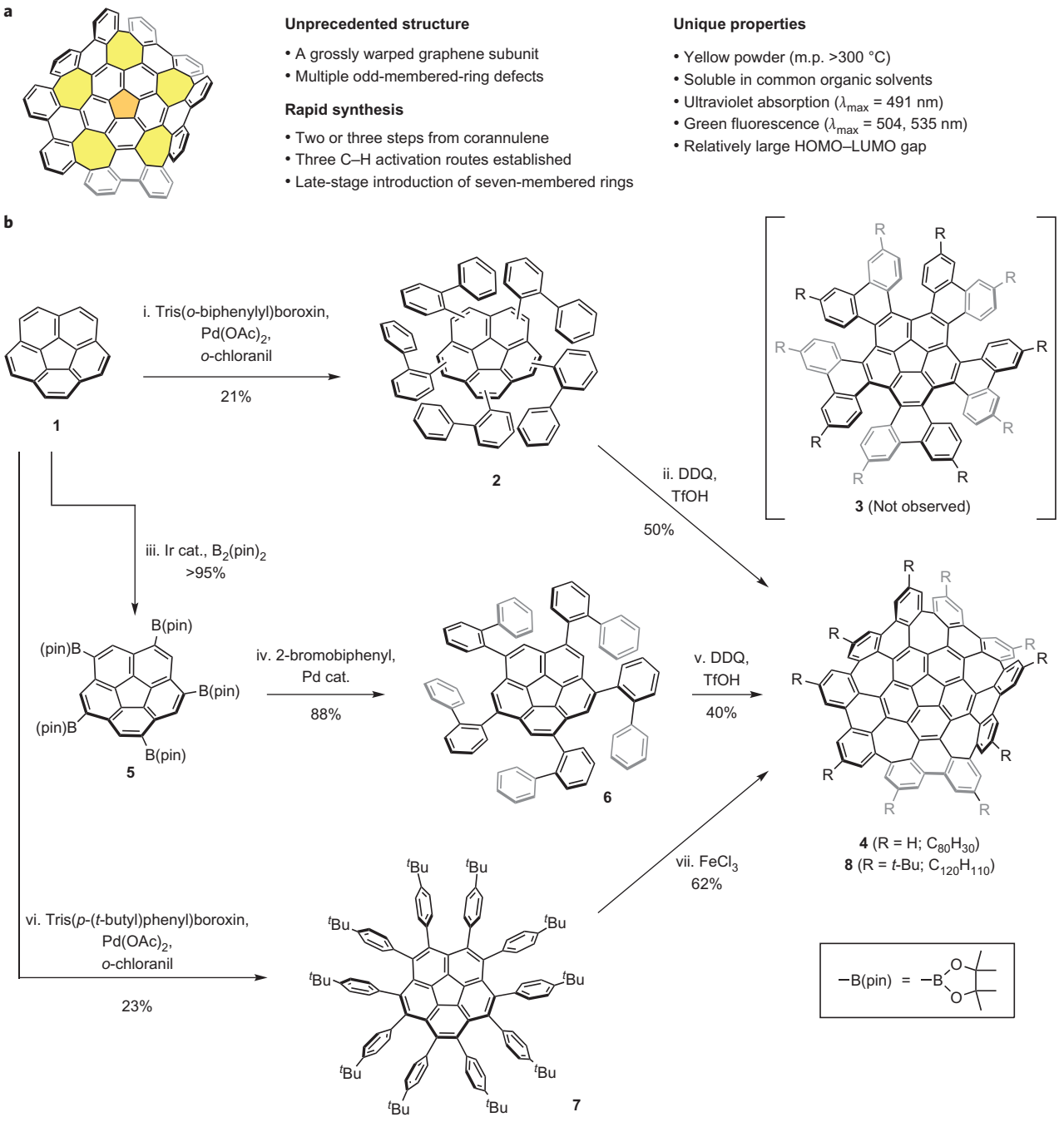

Figure 1 | Structure of 4, its salient properties and three different synthesis methods. a, Important features of the grossly warped $C_{80}H_{30}$ nanographene. **b**, Synthetic routes to $C_{80}H_{30}$ (**4**) and its deca-*t*-butyl derivative $C_{120}H_{110}$ (**8**) from corannulene (**1**). For Route 1, direct fivefold C–H biphenylation, the reaction conditions were (i) tris(*o*-biphenylyl)boroxin (2.0 equiv.), $Pd(OAc)_2$ (20 mol%), *o*-chloranil (5.0 equiv.), DCE, 80 °C, 16 h and (ii) DDQ (10 equiv.), trifluoromethanesulfonic acid (TfOH)/CH_2Cl_2 (5:95), 0 °C, 30 minutes. For Route 2, stepwise fivefold C–H borylation–arylation, the reaction conditions were (iii) $(Ir(OMe)(cod))_2$ (20 mol%), $B_2(pin)_2$ (5.2 equiv.), 4,4′-dimethylbipyridyl (40 mol%), potassium *t*-butoxide (10 mol%), tetrahydrofuran (THF), 85 °C, four days, (iv) 2-bromobiphenyl (20 equiv.), $Pd_2(dba)_3{\cdot}CHCl_3$ (10 mol%), 2-dicyclohexylphosphino-2′,6′-dimethoxybiphenyl (SPhos, 20 mol%), Cs_2CO_3 (10 equiv.), toluene/water (2:1), 80 °C, 24 hours and (v) DDQ (10 equiv.), TfOH/CH_2Cl_2 (5:95), 0 °C, 30 minutes. For Route 3, direct tenfold 'total' C–H phenylation, the reaction conditions were (vi) tris(*p*-(*t*-butyl)phenyl)boroxin, $Pd(OAc)_2$, *o*-chloranil, DCE, 80 °C, repeat for 3–4 cycles and (vii) $FeCl_3$ (31 equiv.), CH_2Cl_2/nitromethane (115:1), 25 °C, one hour. cod, 1,5-cyclooctadiene; pin, pinacol; dba, dibenzylideneacetone; cat., catalyst; DCE, 1,2-dichloroethane; DDQ, 2,3-dichloro-5,6-dicyanobenzoquinone.

hexa[7]circulene[38] under otherwise identical conditions. It is remarkable that our syntheses of this 80-carbon nanographene (Fig. 1b) introduce five new strained seven-membered rings in a single chemical reaction.

An X-ray crystal structure of **4** confirms the distortion caused by the cluster of odd-membered rings in this sheet of carbon atoms (Fig. 2a). Five-membered rings embedded in a hexagonal lattice impart geodesic curvature, as in fullerenes[7,39], but seven-membered rings introduce so-called 'negative curvature'[40]. The dense accumulation of both kinds of odd-membered-ring defects in **4** leads to its unique double-concave structure (Fig. 2b). The central corannulene moiety adopts a shallow bowl-shaped geometry with a bowl depth of

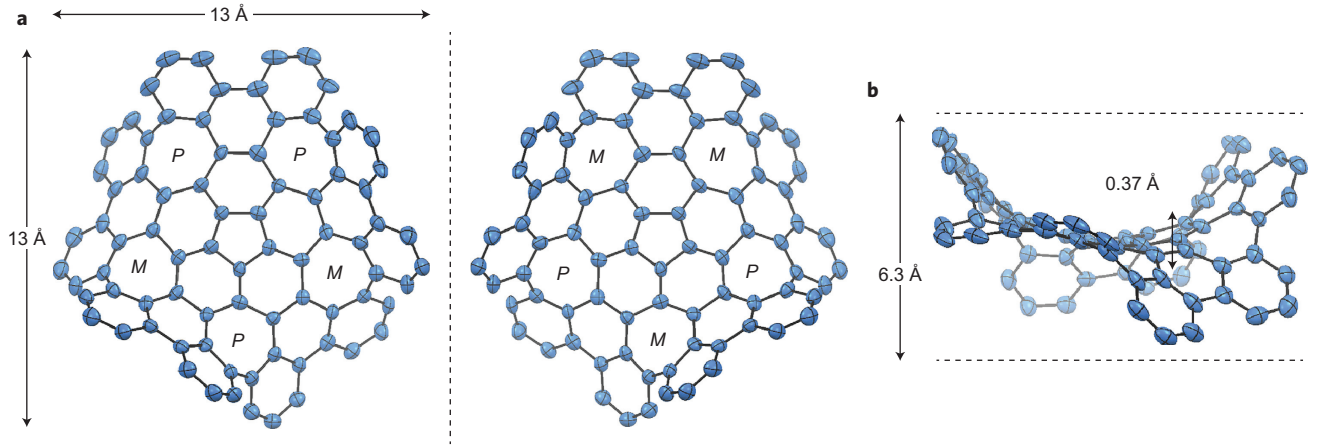

Figure 2 | ORTEP images showing the warped structure of the new $C_{80}H_{30}$ nanographene 4, taken from the X-ray crystal structure. a, Top view of enantiomer pair of **4**, *PMPMP*-isomer (left) and *MPMPM*-isomer (right). **b**, Side view. In the ORTEP images all of the atoms shown are carbons (hydrogen atoms on the perimeter are omitted for clarity) and thermal ellipsoids for the carbon atoms show 50% positional probability.

0.37 Å (Fig. 2b). More interestingly, the presence of five helical hexa[7]circulene moieties[38], each with *M* or *P* chirality around the seven-membered ring, makes **4** a chiral molecule with enantiomers of *MPMPM* and *PMPMP* configuration (Fig. 2a). The strain in this nanographene is manifest in the deformation of so many C–C–C bond angles away from the natural value of 120°; from the X-ray structure of **4**, the C–C–C bond angles are seen to range from 106.0(6)° to 138.3(7)°. To the best of our knowledge, **4** represents the largest PAH, other than fullerenes and their derivatives, whose structure has been determined by X-ray crystallography[41].

The low solubility of graphite, and of even moderately sized planar nanographenes[27–29], stems from the strong van der Waals attraction associated with large-area contacts between adjacent graphene faces. Compounds **4** and **8**, however, lack such large-area contacts with their neighbours in the solid state (see the X-ray crystal packing diagrams in the Supplementary Information) and are soluble in common organic solvents. The *t*-butyl groups on **8** enhance the solubility further[41], and this $C_{120}H_{110}$ hydrocarbon is freely soluble even in hexane!

Though frozen in a single conformation by crystal packing constraints in the solid state, this 26-ring carbon framework is highly flexible in solution and changes its shape constantly. In the static structure (Fig. 2), each of the ten benzo groups around the perimeter of the molecule is structurally distinct from all the others and occupies a unique environment. When unconstrained in solution, however, the molecule can equalize all ten benzo groups around its perimeter, which renders them time-averaged equivalent by rotations around the rim bonds between them and bowl-to-bowl inversion of the central corannulene. Density functional theory (DFT) calculations at the B3LYP/6-31G(d) level of theory predict activation energies of 1.7 and 18.9 kcal mol^{-1}, respectively, for the bowl-to-bowl inversion and the racemization of **4** (Fig. 3a). The barrier calculated for bowl-to-bowl inversion of **4** is considerably lower than that calculated for corannulene (10.4 kcal mol^{-1}) at the same level of theory (Fig. 3b); the best estimate from experiments[42,43] is about 11 kcal mol^{-1}. The shallowness of the bowl in **4** relative to that in the free corannulene molecule (**1**) (bowl depths = 0.37 and 0.87 Å, respectively) is expected to lower the energetic cost for inversion in **4**[42,43].

Evidence for rapid equalization of the ten benzo groups on the perimeter can be seen in the ^{1}H NMR spectrum of **4**, which shows only three signals (a triplet and two doublets), as expected for ten equivalent AMX three-spin systems at 100 °C (Fig. 3d). Rotations around rim bonds sequentially equilibrate the *M* and *P* chiralities of successive hexa[7]circulene moieties at this temperature and send a wave-like motion around the perimeter of the molecule. As the temperature is lowered and bond rotations become slower on the NMR timescale, the coalesced signals broaden. The same behaviour is observed in the variable-temperature ^{1}H NMR spectrum of the deca-*t*-butyl derivative **8** (Fig. 3e). Two coalesced singlets are seen at high temperatures ($\delta = 8.51$ and $\delta = 7.44$ ppm), and they broaden as the solution is cooled. The exceptionally good solubility of this derivative permits the recording of spectra even at −20 °C, at which temperature each of the two singlets splits into five singlets. Line-shape analysis of the variable-temperature NMR spectrum gives experimental values for the activation enthalpy ($\Delta H^{\ddagger}$) and entropy ($\Delta S^{\ddagger}$) associated with this dynamic process of $\Delta H^{\ddagger} = 13.6 \pm 1.5$ kcal mol^{-1} and $\Delta S^{\ddagger} = 0.2 \pm 0.6$ cal mol^{-1} K^{-1}, respectively. The experimental ($\Delta H^{\ddagger}$) value is somewhat smaller than that predicted by molecular orbital calculations for unsubstituted **4** (18.9 kcal mol^{-1}) (Fig. 3a)). The central bowl in **4** continues to invert rapidly even at −20 °C (calculated barrier of only 1.7 kcal mol^{-1}), which explains why the time-averaged symmetry of the molecule drops from D_{5h} to C_2 but not to C_1.

Non-hexagonal-ring defects, particularly the imposition of the seven-membered ring negative curvature, not only cause graphene sheets to warp, but also are predicted to alter their electronic and optical properties[44]. These changes derive not only from non-planarity, but also from changes in connectivity. Unlike all-hexagonal graphene, carbon lattices that contain odd-membered rings are 'non-alternant', and π systems of this class are known to have electronic and optical properties that differ from those of their alternant counterparts (for example, azulene versus naphthalene)[45]. Figure 4a shows a planar, defect-free $C_{78}H_{30}$ nanographene (**9**) synthesized by Müllen and co-workers[46] that compares well in size to the warped $C_{80}H_{30}$ nanographene **4**. DFT calculations at the B3LYP/6-31G(d) level of theory predict that the odd-membered-ring defects cause the energy of the valence band (HOMO) of **4** to drop below that of **9** ($E_{HOMO} = -5.13$ and −4.95 eV, respectively). The conduction bands (LUMOs) of **4** and **9**, however, remain similar ($E_{LUMO} = -2.07$ and −2.05 eV, respectively), which gives the warped nanographene **4** a somewhat wider band gap than that of **9** (3.06 and 2.90 eV, respectively).

Experimentally, the influence of the odd-membered-ring defects on optical properties can be seen in the ultraviolet–visible (UV-vis) absorption spectra of **4** versus that of **9** (Fig. 4b). The β band in the spectrum of the planar nanographene **9** (440 nm) is located at a longer wavelength than that of the warped nanographene **4** (418 nm), and the longest wavelength absorption maximum of **9**

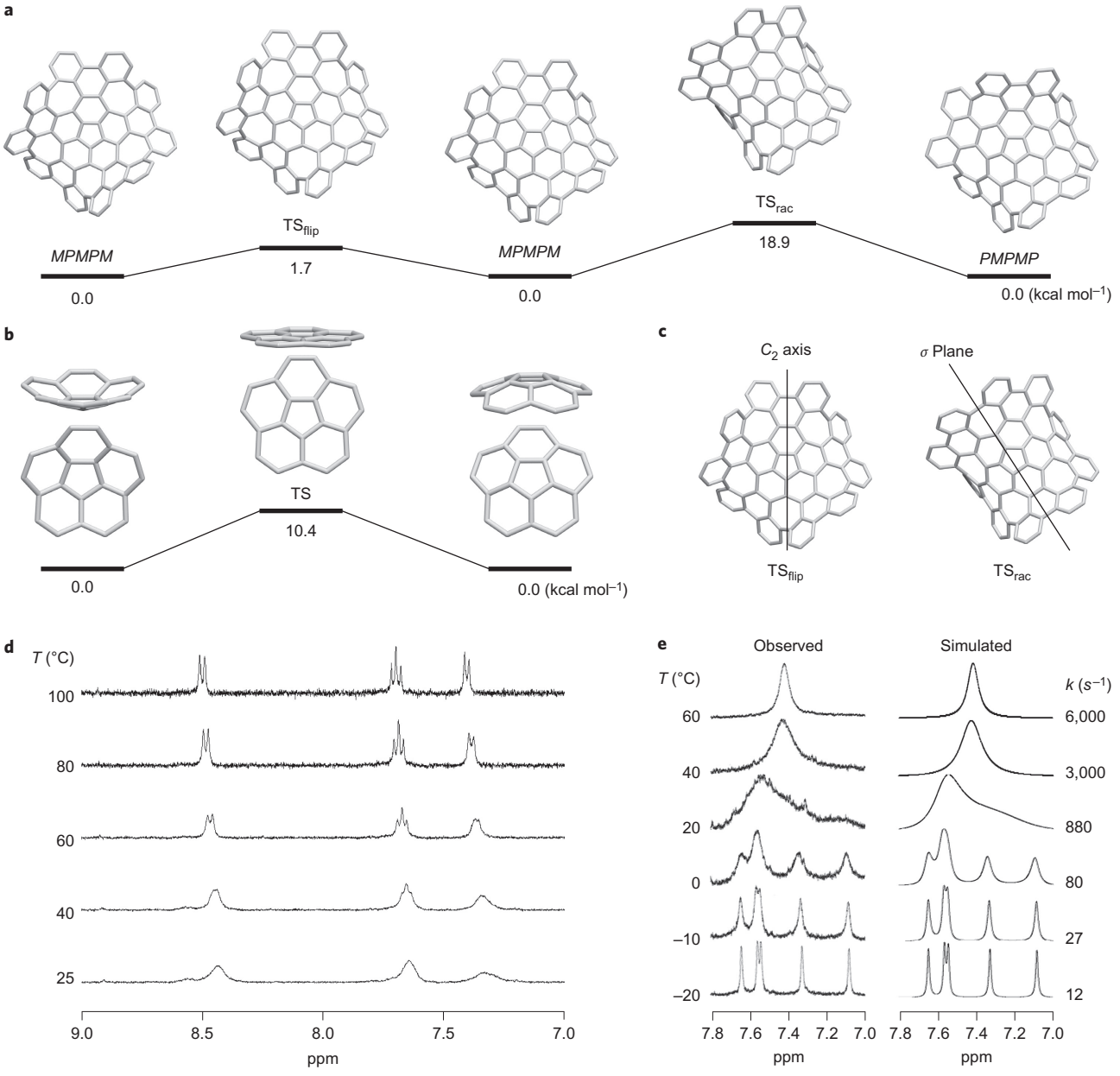

Figure 3 | Conformational flexibility of the grossly warped $C_{80}H_{30}$ nanographene. a, Bowl-to-bowl inversion (left, *MPMPM* ⇔ TS$_{flip}$ ⇔ *MPMPM*) and racemization (right, *MPMPM* ⇔ TS$_{rac}$ ⇔ *PMPMP*) pathways of **4** determined by DFT calculation. Values (kcal mol^{-1}) are relative Gibbs free energies (ΔG) at 298.15 K and 1 atm calculated at the B3LYP/6-31G(d) level of theory. The activation energies of bowl-to-bowl inversion and racemization of **4** are predicted to be 1.7 and 18.9 kcal mol^{-1}, respectively. The bowl-to-bowl inversion barrier of **4** is considerably lower than that of corannulene (**b**). **b**, Pathway and activation energy (10.4 kcal mol^{-1}) of bowl-to-bowl inversion of corannulene determined by DFT calculations at the same level of theory. Both side views and top views of corannulene structures are shown. **c**, C_2 axis and σ plane in the transition states of bowl-to-bowl inversion (TS$_{flip}$) and racemization (TS$_{rac}$) of **4**, respectively. **d**, Variable temperature ^{1}H NMR spectrum of **4** (400 MHz, $C_2D_2Cl_4$) reveals the rapid equalization of the ten benzo groups on the perimeter. **e**, Variable-temperature ^{1}H NMR spectrum of (*t*-Bu)$_{10}C_{80}H_{20}$ **8** (500 MHz, $C_2D_2Cl_4$) gives the experimental values for the activation enthalpy ($\Delta H^{\ddagger} = 13.6 \pm 1.5$ kcal mol^{-1}) and entropy ($\Delta S^{\ddagger} = 0.2 \pm 0.6$ cal mol^{-1} K^{-1}) associated with a wave-like motion around the perimeter of the molecule. *k*, rate constant (s^{-1}).

(shoulder at ~525 nm) lies beyond that of **4** (491 nm). No fluorescence has been reported for **9**, but **4** fluoresces at 504 and 535 nm with a quantum efficiency of 0.26 (see the Supplementary Information).

Moreover, the sufficient solubility of deca-*t*-butyl derivative **8** enabled cyclic voltammetry measurements (see the Supplementary Information). In CH_2Cl_2, **8** displays two reversible oxidations with first and second oxidation potentials of $E_{ox,1} = +0.63$ V and $E_{ox,2} = +0.97$ V versus the ferrocene/ferrocenium couple (Fc/Fc$^+$). In the negative potential region, reversible redox waves were observed at the first, second and third reduction potentials of $E_{red,1} = -1.59$ V, $E_{red,2} = -2.02$ V and $E_{red,3} = -2.31$ V (versus Fc/Fc$^+$). Although a comparison of these cyclic voltammetry data with those of a planar reference system is not possible because planar nanographenes such as **9** are extremely insoluble, a comparison with corannulene (**1**) or fullerenes is interesting. Following the general trend that five-membered rings usually impart good electron-accepting ability, corannulene[47,48] and C_{60} fullerene[49] are reduced easily (up to four- and six-electron reductions, respectively), but are somewhat difficult to oxidize. In contrast, our warped nanographenes can be oxidized easily as well as be

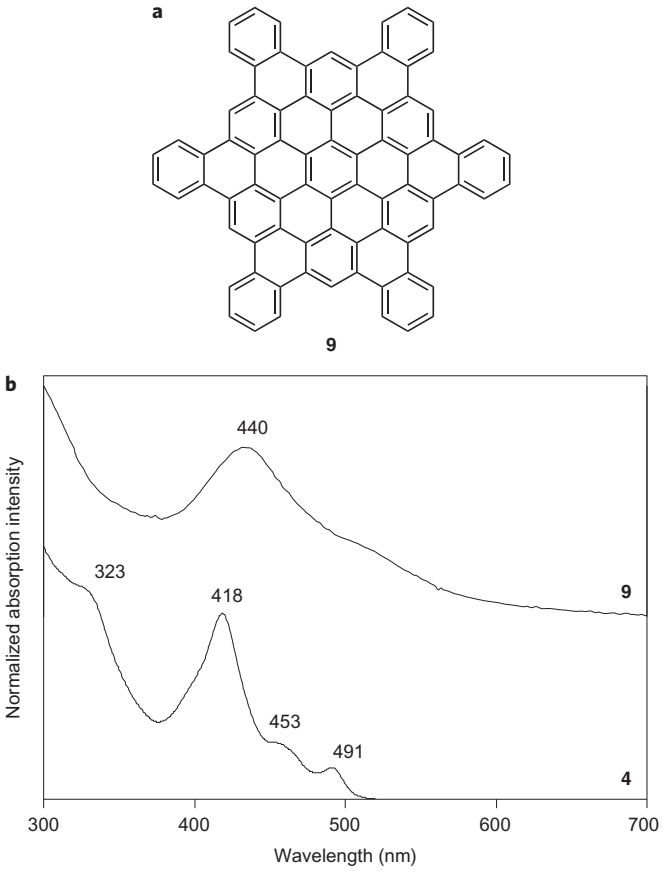

Figure 4 | Optical properties of the grossly warped $C_{80}H_{30}$ nanographene (4) compared to those of a planar PAH of similar size. a, Structure of a planar, defect-free $C_{78}H_{30}$ comparison hydrocarbon **9**. **b**, UV-vis absorption spectra of **4** ($C_{80}H_{30}$) and of the comparison hydrocarbon **9**. The β band and the longest wavelength absorption maximum of **4** (418 nm and 491 nm, respectively) are located at shorter wavelengths than those of **9** (440 nm and ~525 nm, respectively), which indicates that the warped nanographene **4** has a wider band gap than the planar analogue **9**.

reduced (up to three-electron reductions). These properties might be the consequence of having both five- and seven-membered rings in a pentaheptafulvalene form in the molecules.

The $C_{80}H_{30}$ nanographene reported here (**4**) and its deca-*t*-butyl derivative (**8**) provide valuable insights into the effects of multiple odd-membered-ring defects in a graphene sheet. The otherwise planar nanographene becomes grossly warped, as shown by X-ray crystallography. That warping causes dramatic improvements in the solubility properties of the material and also perturbs both the electronic properties and the optical properties. Although rigid and chiral in the solid state, nanographenes **4** and **8** racemize rapidly in solution by a novel dynamic process that was modelled computationally. The ease with which this remarkable ring system can be synthesized in just two steps testifies to the power of modern C–H activation chemical methods. To date, the 26-ring nanographene **4** is the largest PAH, other than fullerenes and their derivatives, to have been characterized by X-ray crystallography.

Methods

Fivefold C–H arylation of corannulene. A solution of $Pd(OAc)_2$ (4.5 mg, 20 μmol, 20 mol%), *o*-chloranil (122 mg, 0.50 mmol, 5.0 equiv.), corannulene (**1**: 25 mg, 0.10 mmol, 1.0 equiv.) and tris(*o*-biphenylyl)boroxin (108 mg, 0.20 mmol, 2.0 equiv.) in dry 1,2-dichloroethane (DCE) (10 ml) was stirred at 80 °C for 16 hours under argon. The reaction mixture was then passed through a pad of silica gel with copious washings with CH_2Cl_2 (50 ml). The filtrate was concentrated and subjected to silica-gel column chromatography (eluent, hexane/CH_2Cl_2 = 100:0 to 80:20) to give pentakis(*o*-biphenylyl)corannulene (**2**: 23 mg, 21% yield) as a mixture of regioisomers.

Synthesis of $C_{80}H_{30}$. To a solution of pentakis(*o*-biphenylyl)corannulene (**2**, 10 mg, 10 μmol, 1.0 equiv.) in dry CH_2Cl_2 (1.9 ml) was added 2,3-dichloro-5,6-dicyanobenzoquinone (DDQ, 23 mg, 0.1 mmol, 10 equiv.) at 0 °C. After stirring for five minutes, trifluoromethanesulfonic acid (0.1 ml) was added to the mixture. The mixture was further stirred for 30 minutes at 0 °C. The reaction mixture was neutralized with saturated aqueous $NaHCO_3$ and then extracted with CH_2Cl_2. The combined organic phase was dried over $MgSO_4$ and the organic solvent was removed under reduced pressure. The residue was then dissolved into tetrachloroethane and incubated at 100 °C for 30 minutes. The thus-obtained precipitate was collected by filtration and the residue was dried under vacuum to afford $C_{80}H_{30}$ (**4**, 4.9 mg, 50% yield) as a yellow powder. Recrystallization of **4** from hot 1,1,2,2-tetrachloroethane yielded yellow crystals of $C_{80}H_{30}{\cdot}2C_2H_2Cl_4$ suitable for X-ray crystal structure analysis. Details of the crystal data and a summary of the intensity data collection parameters for $C_{80}H_{30}$ are listed in the Supplementary Information. CCDC 919707 contains the supplementary crystallographic data for this paper. These data can be obtained free of charge from The Cambridge Crystallographic Data Centre via www.ccdc.cam.ac.uk/data_request/cif.

Received 7 February 2013; accepted 5 June 2013; published online 14 July 2013

References

1. Kroto, H. W., Heath, J. R., O'Brien, S. C., Curl, R. F. & Smalley, R. E. C_{60}: buckminsterfullerene. *Nature* **318,** 162–163 (1985).
2. Iijima, S. Helical microtubules of graphitic carbon. *Nature* **354,** 56–58 (1991).
3. Novoselov, K. S. *et al.* Electric field effect in atomically thin carbon films. *Science* **306,** 666–669 (2004).
4. Akasaka, T., Wudl, F. & Nagase, S. (eds) *Chemistry of Nanocarbons* (Wiley, 2010).
5. Chen, X., Engle, K. M., Wang, D-H. & Yu, J-Q. Pd(II)-catalyzed C–H activation/C–C cross-coupling reactions: versatility and practicality. *Angew. Chem. Int. Ed.* **48,** 5094–5115 (2009).
6. Yamaguchi, J., Yamaguchi, A. D. & Itami, K. C–H bond functionalization: emerging synthetic tools for natural products and pharmaceuticals. *Angew. Chem. Int. Ed.* **51,** 8960–9009 (2012).
7. Tsefrikas, V. M. & Scott, L. T. Geodesic polyarenes by flash vacuum pyrolysis. *Chem. Rev.* **106,** 4868–4884 (2006).
8. Scott, L. T. Fragments of fullerenes: novel syntheses, structures, and reactions. *Pure Appl. Chem.* **68,** 291–300 (1996).
9. Scott, L. T. *et al.* Geodesic polyarenes with exposed concave surfaces. *Pure Appl. Chem.* **71,** 209–221 (1999).
10. Scott, L. T. Polycyclic aromatic hydrocarbon bowls, baskets, balls, and tubes: challenging targets for chemical synthesis. *Polycycl. Aromat. Compd* **30,** 247–259 (2010).
11. Wu, Y-T. & Siegel, J. S. Aromatic molecular-bowl hydrocarbons: synthetic derivatives, their structures, and physical properties. *Chem. Rev.* **106,** 4843–4867 (2006).
12. Sygula, A. & Rabideau, P. W. in *Carbon-Rich Compounds* (eds Haley, M. M. & Tykwinski, R. R.) 529–565 (Wiley-VCH, 2006).
13. Mehta, G. & Rao, H. S. P. Synthetic studies directed towards bucky-balls and bucky-bowls. *Tetrahedron* **54,** 13325–13370 (1998).
14. Petrukhina, M. A. & Scott, L. T. *Fragments of Fullerenes and Carbon Nanotubes: Designed Synthesis, Unusual Reactions, and Coordination Chemistry* (Wiley, 2011).
15. Hirst, E. S. & Jasti, R. Bending benzene: synthesis of [*n*]cycloparaphenylenes. *J. Org. Chem.* **77,** 10473–10478 (2012).
16. Omachi, H., Segawa, Y. & Itami, K. Synthesis of cycloparaphenylenes and related carbon nanorings: a step toward the controlled synthesis of carbon nanotubes. *Acc. Chem. Res.* **45,** 1378–1389 (2012).
17. Jasti, R., Bhattacharjee, J., Neaton, J. B. & Bertozzi, C. R. Synthesis, characterization, and theory of [9]-, [12]-, and [18]cycloparaphenylene: carbon nanohoop structures. *J. Am. Chem. Soc.* **130,** 17646–17647 (2008).
18. Takaba, H., Omachi, H., Yamamoto, Y., Bouffard, J. & Itami, K. Selective synthesis of [12]cycloparaphenylene. *Angew. Chem. Int. Ed.* **48,** 6112–6116 (2009).
19. Omachi, H., Matsuura, S., Segawa, Y. & Itami, K. A modular and size-selective synthesis of [*n*]cycloparaphenylenes: a step toward the selective synthesis of [*n*,*n*]single-walled carbon nanotubes. *Angew. Chem. Int. Ed.* **49,** 10202–10205 (2010).
20. Ishii, Y. *et al.* Size-selective synthesis of [9]–[11] and [13]cycloparaphenylenes. *Chem. Sci.* **3,** 2340–2345 (2012).
21. Iwamoto, T., Watanabe, Y., Sakamoto, Y-I., Suzuki, T. & Yamago, S. Selective and random syntheses of [*n*]cycloparaphenylenes ($n = 8$–13) and size dependence of their electronic properties. *J. Am. Chem. Soc.* **133,** 8354–8361 (2011).

22. Hitosugi, S., Yamasaki, T. & Isobe, H. Bottom-up synthesis and thread-in-bead structures of finite (*n*,0)-zigzag single-wall carbon nanotubes. *J. Am. Chem. Soc.* **134,** 12442–12445 (2012).
23. Nishiuchi, T., Feng, X., Enkelmann, V., Wagner, M. & Müllen, K. Three-dimensionally arranged cyclic *p*-hexaphenylbenzene: toward a bottom-up synthesis of size-defined carbon nanotubes. *Chem. Eur. J.* **18,** 16621–16625 (2012).
24. Yagi, A., Segawa, Y. & Itami, K. Synthesis and properties of [9]cyclo-1,4-naphthylene: a π-extended carbon nanoring. *J. Am. Chem. Soc.* **134,** 2962–2965 (2012).
25. Matsui, K., Segawa, S., Namikawa, T., Kamada, K. & Itami, K. Synthesis and properties of all-benzene carbon nanocages: a junction unit of branched carbon nanotubes. *Chem. Sci.* **4,** 84–88 (2013).
26. Omachi, H., Nakayama, T., Takahashi, E., Segawa, Y. & Itami, K. Initiation of carbon nanotube growth by well-defined carbon nanorings. *Nature Chem.* http://dx.doi.org/10.1038/nchem.1655 (2013).
27. Watson, M. D., Fechtenkoetter, A. & Müllen, K. Big is beautiful – 'aromaticity' revisited from the viewpoint of macromolecular and supramolecular benzene chemistry. *Chem. Rev.* **101,** 1267–1300 (2001).
28. Feng, X., Pisula, W. & Müllen, K. Large polycyclic aromatic hydrocarbons: synthesis and discotic organization. *Pure Appl. Chem.* **81,** 2203–2224 (2009).
29. Chen, L., Hernandez, Y., Feng, X. & Müllen, K. From nanographene and graphene nanoribbons to graphene sheets: chemical synthesis. *Angew. Chem. Int. Ed.* **51,** 7640–7654 (2012).
30. Scott, L. T. *et al.* A rational chemical synthesis of C_{60}. *Science* **295,** 1500–1503 (2002).
31. Scott, L. T. *et al.* A short, rigid, structurally pure carbon nanotube by stepwise chemical synthesis. *J. Am. Chem. Soc.* **134,** 107–110 (2012).
32. Mochida, K., Kawasumi, K., Segawa, Y. & Itami, K. Direct arylation of polycyclic aromatic hydrocarbons through palladium catalysis. *J. Am. Chem. Soc.* **133,** 10716–10719 (2011).
33. Eliseeva, M. N. & Scott, L. T. Pushing the Ir-catalyzed C–H polyborylation of aromatic compounds to maximum capacity by exploiting reversibility. *J. Am. Chem. Soc.* **134,** 15169–15172 (2012).
34. Zhang, Q., Kawasumi, K., Segawa, Y., Itami, K. & Scott, L. T. Palladium-catalyzed C–H activation taken to the limit. Flattening an aromatic bowl by total arylation. *J. Am. Chem. Soc.* **134,** 15664–15667 (2012).
35. Dopper, J. H., Oudman, D. & Wynberg, H. Dehydrogenation of heterohelicenes by a Scholl type reaction. Dehydrohelicenes. *J. Org. Chem.* **40,** 3398–3401 (1975).
36. Mughal, E. U. & Kuck, D. Merging tribenzotriquinacene with hexa-*peri*-hexabenzocoronene: a cycloheptatriene unit generated by Scholl reaction. *Chem. Commun.* **48,** 8880–8882 (2012).
37. Pradhan, A., Dechambenoit, P., Bock, H. & Durola, F. Twisted polycyclic arenes by intramolecular Scholl reactions of C3-symmetric precursors. *J. Org. Chem.* **78,** 2266–2274 (2013).
38. Jessup, P. J. & Reiss, J. A. Cyclophanes, V. Biphenylnaphthalenophanes and the synthesis of hexa[7]circulene. *Aust. J. Chem.* **29,** 173–176 (1976).
39. Bharat *et al.* Quadrannulene: a nonclassical fullerene fragment. *Angew. Chem. Int. Ed.* **49,** 399–402 (2010).
40. King, R. B. Chemical applications of topology and group theory. 29. Low density polymeric carbon allotropes based on negative curvature structures. *J. Phys. Chem.* **100,** 15096–15104 (1996).
41. Kumar, B., Strasser, C. E. & King, B. T. *t*-Butyl biphenylation of *o*-dibromoarenes: a route to soluble polycyclic aromatic hydrocarbons. *J. Org. Chem.* **77,** 311–316 (2012).
42. Seiders, T. J., Baldridge, K. K., Grube, G. H. & Siegel, J. S. Structure/energy correlation of bowl depth and inversion barrier in corannulene derivatives: combined experimental and quantum mechanical analysis. *J. Am. Chem. Soc.* **123,** 517–525 (2001).
43. Scott, L. T., Hashemi, M. M. & Bratcher, M. S. Corannulene bowl-to-bowl inversion is rapid at room temperature. *J. Am. Chem. Soc.* **114,** 1920–1921 (1992).
44. Kapko, V., Drabold, D. A. & Thorpe, M. F. Electronic structure of a realistic model of amorphous graphene. *Phys. Status Solidi B* **247,** 1197–1200 (2010).
45. Michl, J. & Thulstrup, E. W. Why is azulene blue and anthracene white? A simple MO picture. *Tetrahedron* **32,** 205–209 (1976).
46. Doetz, F., Brand, J. D., Ito, S., Gherghel, L. & Müllen, K. Synthesis of large polycyclic aromatic hydrocarbons: variation of size and periphery. *J. Am. Chem. Soc.* **122,** 7707–7717 (2000).
47. Janata, J. *et al.* Concerning the anion and cation radicals of corannulene. *J. Am. Chem. Soc.* **89,** 3056–3058 (1967).
48. Bruno, C. *et al.* Electrochemical and theoretical investigation of corannulene reduction processes. *J. Phys. Chem. B* **113,** 1954–1962 (2009).
49. Yang, Y. *et al.* Reversible fullerene electrochemistry: correlation with the HOMO–LUMO energy difference for C_{60}, C_{70}, C_{76}, C_{78}, and C_{84}. *J. Am. Chem. Soc.* **117,** 7801–7804 (1995).

Acknowledgements

K.K. thanks the Japan Society for the Promotion of Science (JSPS) and the Nagoya University Global Center of Excellence Program for fellowships. This research was supported financially by the US National Science Foundation (L.T.S.) and the Funding Program for Next Generation World-Leading Researchers from JSPS (K.I.). We thank Mr T. Fujikawa for conducting the reactions of [6]helicene. K. Tatsumi and Y. Ohki are greatly acknowledged for providing access to their X-ray analysis instruments. We thank S. Yamaguchi, A. Fukazawa and S. Saito for assistance in the photophysical measurements. S. Seki and A. Saeki are acknowledged for measurements and discussion. Calculations were performed using the resources of the Research Center for Computational Science, Okazaki, Japan.

Author contributions

K.K. and Q.Z conducted the experiments. Y.S. performed the X-ray crystal structure analysis and DFT calculations. L.T.S. and K.I. conceived the concept and prepared the manuscript with feedback from others.

Additional information

Supplementary information and chemical compound information are available in the online version of the paper. Reprints and permissions information is available online at www.nature.com/reprints. Correspondence and requests for materials should be addressed to L.T.S. and K.I.

Competing financial interests

The authors declare no competing financial interests.